


Net energy up-conversion processes in CdSe/CdS (core/shell) quantum dots: A possible pathway towards optical cooling

Muchuan Hua  and Ricardo S. Decca *

Department of Physics, Indiana University–Purdue University Indianapolis, Indianapolis, Indiana 46202, USA

 (Received 28 March 2022; revised 1 August 2022; accepted 2 August 2022; published 25 August 2022)

An investigation of the possibility of optical refrigeration (OR) on zinc-blende cadmium selenide/cadmium sulfide (CdSe/CdS) core/shell structure quantum dots (QDs) has been carried out. Quality samples were synthesized in our laboratory, and significant energy up-conversion photoluminescence (UCPL) was observed in these samples, showing the potential of generating net cooling effects. To better understand and predict the UCPL characteristics of the QDs, a semiempirical model has been developed, showing good agreement with our experimental results. The model takes into account the corresponding quantum yield and cooling efficiency, predicting the possibility of realizing optical refrigeration on a CdSe QD system.

DOI: [10.1103/PhysRevB.106.085421](https://doi.org/10.1103/PhysRevB.106.085421)

I. INTRODUCTION

The idea of optical refrigeration (OR) in solids was first proposed by Pringsheim in 1929. He suggested that the thermal vibration energy in solids can be removed by spontaneous anti-Stokes (energy up-conversion) photoluminescence (PL), where the mean emission energy $\bar{\epsilon}_{\text{em}}$ is higher than the energy of the excitation light ϵ_{ex} [1]. However, implementations of this technique are very limited, and most of them are in rare-earth-ion-doped glass systems [2–11]. In 2012, Zhang *et al.* showed the possibility of realizing OR in semiconducting nanomaterials [12]. In their experiment, CdS nanobelts were cooled by 40 K under laser light. It is attractive to test OR in other semiconducting nanomaterials, such as semiconducting quantum dots (QDs). Semiconducting QDs are well known for their optical properties due to the “quantum size effect,” i.e., quantization of the absorption spectra and size-tunable energy band gap [13]. These phenomena allow wide applications of semiconducting QDs in light-emitting and photovoltaic devices [14–16]. It would be attractive to use the tunable energy gap and “atomiclike” emission spectra from QDs to achieve OR, particularly when considering their large absorption cross section. Besides being a natural extension to the work done in CdS nanobelts, QDs would provide a much more versatile platform for OR since it is simpler to prepare them in suspension or in a solid matrix [12].

To achieve OR in a material, the cooling efficiency η_c ,

$$\eta_c = \eta_{\text{abs}} \eta_{\text{ext}} \frac{\bar{\epsilon}_{\text{em}}}{\epsilon_{\text{ex}}} - 1, \quad (1)$$

must be positive [8]. Here η_{abs} is the absorption efficiency of the system, defined as $\eta_{\text{abs}} = \frac{\alpha(\epsilon_{\text{ex}}, T)}{\alpha(\epsilon_{\text{ex}}, T) + \alpha_{\text{b}}(\epsilon_{\text{ex}}, T)}$, where $\alpha(\epsilon_{\text{ex}}, T)$ and $\alpha_{\text{b}}(\epsilon_{\text{ex}}, T)$ denote the cooling material and system background’s light absorption rates, respectively. $\eta_{\text{ext}} = \eta \eta_{\text{es}}$, where η denotes the PL quantum yield (QY) of the system,

while η_{es} is the PL escape efficiency, defined as the likelihood of an emitted photon leaving the system. By considering a fairly optimized system, where both η_{abs} and η_{ext} approach unity, Eq. (1) becomes

$$\eta_c \approx \eta \frac{\bar{\epsilon}_{\text{em}}}{\epsilon_{\text{ex}}} - 1. \quad (2)$$

Consequently, a nearly unity QY and net energy up-conversion (UC) during PL processes are critical to realizing OR. However, since QDs’ sizes are typically comparable to their lattice size (a few to tens of lattice parameters along each axis), uncoordinated atoms usually exist on QDs’ surfaces, which form ion traps (also known as surface traps) [17–21]. These surface traps have long trapping lifetimes and favor nonradiative decay processes, introducing a significant drawback in QDs’ QY [22,23]. Therefore, OR was considered unlikely in QDs. Around 2015, multiple breakthroughs were made in CdSe/CdS (core/shell structure) QD synthesis, and samples with a QY close to unity were produced [24,25]. According to Refs. [24–26], complete surface passivation on CdSe QDs was achieved by coating them with a CdS shell, followed by extra ligand treatment. These reports increase the likelihood of realizing OR in CdSe/CdS QDs.

This work focuses on another important criterion for OR, the capability of generating net energy UC during PL processes in CdSe QDs. Typical PL spectra of QDs are obtained with excitation energy ϵ_{ex} much higher than the QD’s absorption band edge (referred to as HPL spectra), where the radiative recombinations of excitons are mostly through the QDs’ intrinsic electronic states (known as electronic band states) [12,27–33]. In contrast, to realize OR in a solid system, for instance, Yb³⁺-doped glass, ϵ_{ex} is expected to be the lowest allowed absorption energy, such that the state density distribution (SDD) favors the energy UC processes, as energy down-conversion (DC) processes are always thermally more favorable. In the case of QDs, their HPL spectra are universally redshifted from the absorption edge at noncryogenic temperature, meaning ϵ_{ex} needs to be much lower (depending

*rdecca@iupui.edu

on the materials and size of the QDs, typically, about 80 meV for CdSe/CdS QDs) than the absorption band edge in order to generate net energy UC [34–36]. The existence of such up-conversion photoluminescence (UCPL) processes in group II-VI QDs was previously observed, and the QDs' surface states [37] and interfacial states between the core and the coating shell [38] were concluded to be the origins of the UCPL processes [37–41]. As the whole synthesizing procedure to produce near-unity QY colloidal QDs ties to removing the internal and surface defects, such UCPL processes could also be completely prohibited [25,26]. Thus, characterizing the high-quality CdSe/CdS QDs' PL properties with subband excitation (SBE) is crucial to OR. In this work, zinc-blende CdSe QDs coated with zinc-blende CdS shells were synthesized. They were reported to have almost unity QY and to be mass production friendly, allowing their wide application [26,42,43]. Based on the experimental data collected with these samples, a phenomenological model to describe the UCPL processes in zinc-blende CdSe/CdS QDs is proposed to help estimate the possible cooling efficiency that such QD systems could achieve. In Sec. II details of the experimental techniques for sample characterization and the apparatus used in obtaining PL data are discussed. Special emphasis is placed on the modifications from usual PL systems that permit the collection of the PL signal in the samples. In Sec. III the obtained experimental data are shown. In Sec. IV the model for the recombination processes based on the experimental results is presented, and a different dimensionality for the vibrational modes is considered. Finally, in Sec. V the conclusions of our work are presented.

II. EXPERIMENTAL SETUP

Experimental data were obtained from CdSe/CdS core/shell structure QD samples prepared in our laboratory. Synthesis of the samples was carried out in two stages: synthesis of CdSe seeds and growth of the CdS shell. The method for seed synthesis is well documented [44]; the shell growth was accomplished by using a single precursor (cadmium diethyldithiocarbamate) with an adhesion-growth method [26], and outside the CdS shell, a monolayer of cadmium formate was applied to passivate the shell surface [25,45].

Absorption spectra of the samples were obtained by using a Thermal Scientific Evolution 600 UV-Vis spectrometer. PL spectra of the QD samples were obtained with a Horiba Triax 550 monochromator equipped with a LN₂-cooled CCD chip (CCD 3000). A HeNe laser with an emission peak at 1.957 eV, a laser diode with a tunable emission energy range of 1.919–1.945 eV, and another laser diode with a typical emission energy of 3.06 eV were used as the excitation sources.

The common difficulty of observing QD samples' PL spectra at SBE is that the excitation energies are within the range of the PL emission spectra and have an extremely low absorption efficiency, such that the PL signal is overwhelmed by the scattered laser signal. For our application, a full PL line shape evaluation is critical as the possible cooling efficiency is directly related to the spectral profile. In order to increase the PL-to-laser-signal ratio, an off-axis-collecting system was used. As shown in Fig. 1, the PL light of the QD sample

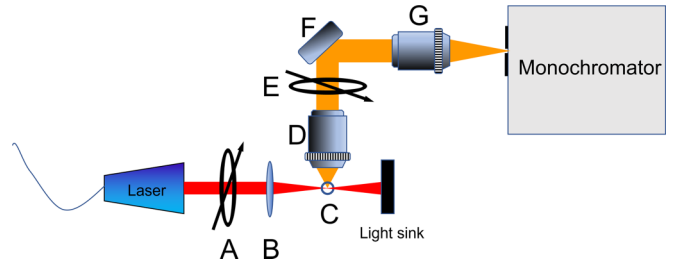


FIG. 1. Schematic plot of the off-axis collecting system: A: polarizer, B: focusing lens, C: sample holder, D: collection objective, E: analyzer, F: highly reflective mirror, G: adapting objective.

was collected perpendicularly to the incident laser. To further suppress the scattered excitation light, a pair of linear polarizers was introduced. The mechanism of the system is based on the fact that the PL property of zinc-blende (cubic crystal structure) CdSe QDs has no polarization preference, but the strength of the laser light does (dominated by the Rayleigh scattering). Thus, two polarizers were introduced in the excitation and collection paths separately (parts A and E in Fig. 1) to utilize the difference between their polarization properties. One of them was placed right before the focusing lens to horizontally polarize the incident laser light. The other one was used as an analyzer, placed right above the collection objective with its polarization direction aligned with the incident laser beam. Although in such a configuration the collecting objective is aligned with the direction of the maximized scattering strength, the polarization of the scattered light is preferentially perpendicular to the analyzer. Experimentally, an extinction ratio of about 127:1 was typically achieved. The usual excitation power was less than 300 μ W (around 600 W/cm²), such that the mean excitonic density in each QD is much less than 1, precluding multiphoton processes.

III. EXPERIMENTAL DATA

The basic optical properties of the samples are listed in Table I. Samples 1 to 3 were produced from the same batch, while sample 4 was obtained from another batch. Before the shells were grown, core sizes were calculated using a semiempirical equation from Ref. [46], where a value of 3.0 nm was derived for samples 1 to 3 and a value of 3.3 nm was derived for sample 4. The samples' absorption spectra showed clear features of energy quantization [a typical absorption spectrum is shown in Fig. 2(a)], indicating the successful synthesis of QDs. The PL FWHM is less than 90 meV, while the HPL spectra show rapid decay on both the high- and low-energy

TABLE I. PL information of the QDs samples.

Sample	Shell thickness (monolayers)	First absorption maximum (eV)	HPL peak energy (eV)	FWHM (meV)
1	2		2.067	89
2	4		2.027	89
3	4 + CdFt ^a	2.059	2.023	87
4	4 + CdFt	2.049	2.011	81

^aThe surface of the CdS is passivated with a monolayer of CdFt.

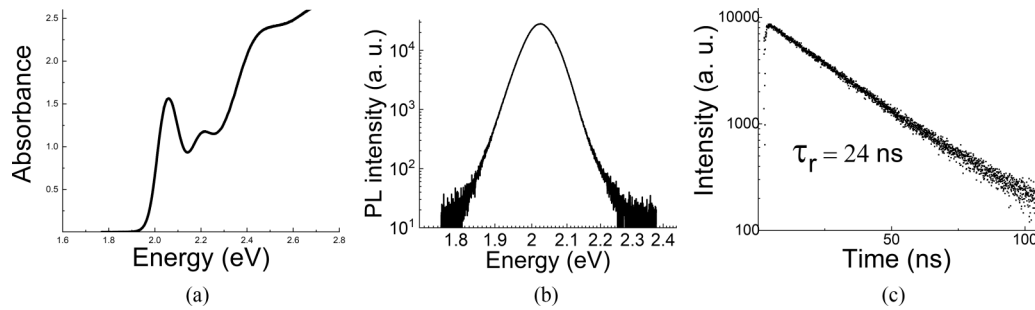


FIG. 2. (a) Absorption spectrum of the sample. (b) High-energy excitation PL spectrum in logarithmic scale ($\epsilon_{\text{ex}} = 3.06$ eV). (c) Time-dependent radiative decay intensity curve of the QD sample. The curve was fitted with a single exponential curve with a decay lifetime $\tau = 24$ ns. All the data shown were collected with sample 3.

sides [Fig. 2(b)], indicating a good monodispersity of the QD size distribution [43,47]. Furthermore, the absence of the deep trap emission around 1.8 eV indicates nearly complete passivation of the core surface [48]. Figure 2(c) shows the radiative decay lifetime, yielding a single exponential curve, confirming the report from Peng's group [26], in which unity QY was achieved in their QD samples after complete surface passivation and a single radiative decay lifetime was observed. Hence, these QDs are suitable candidates for investigating specific transitions involved in UCPL.

With the help of the off-axis collection system, the laser signal within the spectrum is significantly reduced. As seen in Fig. 3(a), only a small “spike” around the laser energy was observed in the much larger PL signal. Furthermore, the spike was found to be more noticeable at lower excitation energy, where absorption efficiency is lower, indicating it does not originate from PL processes. Therefore, we conclude such spikes originated from the scattered laser light, and the samples' PL spectra with SBE have a smooth line shape with a single peak. As shown in Fig. 3(b), the sample's PL intensity is linearly dependent on the excitation intensity, indicating, as mentioned before, that multiphoton absorption processes make a negligible contribution. More importantly for our work, a significant UCPL signal was observed in our sample, which is a prerequisite for OR [see Fig. 3(a)].

Such UCPL was observed by Rusakov *et al.* [38] and Wang *et al.* [37] within CdSe/ZnS and CdTe colloidal QDs, respectively. Each group proposed a mechanism which is different from the other one to explain the observed UCPL processes.

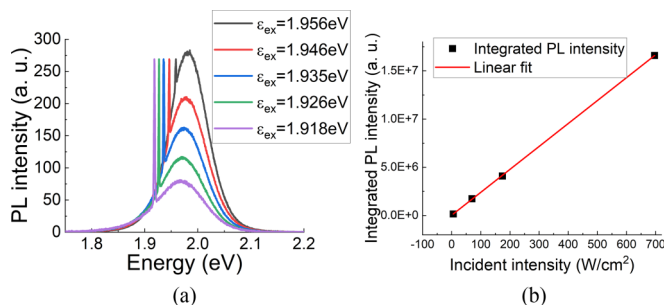


FIG. 3. (a) Excitation-energy-dependent PL spectra (PL intensities were normalized with respect to the observed laser signals) of sample 3. (b) Excitation intensity dependence of the PL intensity of sample 4 at $\epsilon_{\text{ex}} = 1.941$ eV. The line is a linear fit to the data.

In Ref. [38], the UCPL processes in CdSe/ZnS QDS were concluded to originate from the trapping states introduced by the interfacial lattice disorder as the UCPL intensity was enhanced with a thicker ZnS shell. However, several issues were found when applying this model to our samples: First, lattice mismatch between zinc-blende CdS and zinc-blende CdSe (3.6%) is much smaller than the case of zinc-blende ZnS and zinc-blende CdSe (10.6%), leading to a much lower chance of introducing interfacial disorder. Second, CdSe/CdS QDs' intrinsic energy gap is supposed to have a strong shell thickness dependence. To address the shell thickness issue, we compare the PL spectra of sample 2 (sample with a four-monolayer-thick CdS shell) with those of sample 1 (with a two-monolayer shell). As shown in Fig 4(a), however, the HPL peak energy is shifted from 2.067 to 2.027 eV after increasing the CdS shell thickness from two to four monolayers. Therefore, a potential enhancement observed with a fixed excitation energy could be a consequence of the increased band-edge absorption due to the thicker shell. To minimize the effect due to the shifting in the QDs' intrinsic energy band gap, a comparison was made between the two samples' PL spectra excited with laser energies lowered by an equal amount with respect to their own HPL peak energies. As shown in Fig. 4(b), with excitation energies around 90 meV lower than their HPL peak energies, in both samples the UCPL spectra peaked about

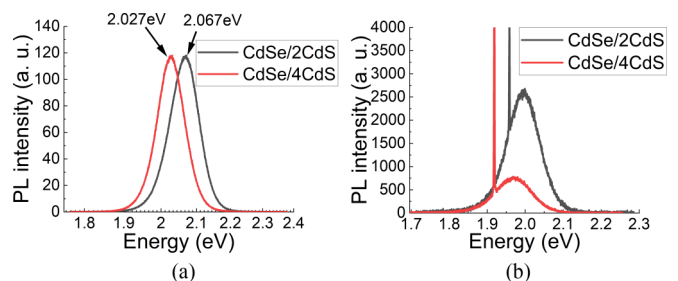


FIG. 4. (a) HPL spectra of CdSe/2CdS (right) and CdSe/4CdS (left) samples. The intensities are adjusted to match each other for easy comparison; both samples were not finished with CdFt. (b) PL spectra of CdSe/2CdS (top) and CdSe/4CdS (bottom) samples excited at 1.956 eV (91 meV lower than the HPL peak energy) and 1.918 eV (89 meV lower than its HPL peak energy), respectively. The PL intensities were normalized by their excitation intensities.

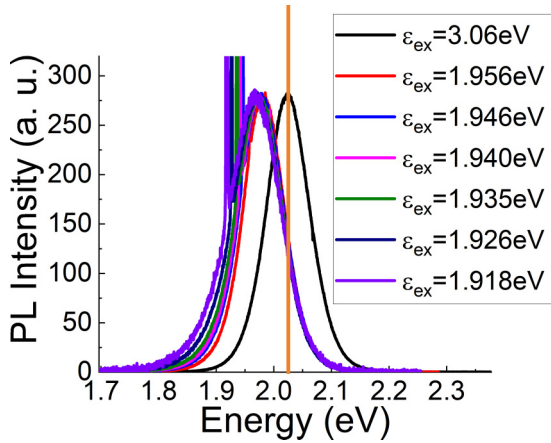


FIG. 5. PL spectra of sample 3 with excitation energies at 3.05 eV, 1.956 eV, 1.946 eV, 1.940 eV, 1.935 eV, 1.926 eV, and 1.918 eV (from right to left). For ease of comparison spectral intensities were adjusted to have the same maximum value. The energy of the HPL maximum is marked by the vertical line.

40 meV above the excitation energies, suggesting UCPL's size dependence is identical to the HPL. At the same time, the PL intensity drops significantly as the shell thickness increases, while an increase in the interfacial disorder is expected. Such observations negate the hypothesis that the UCPL originates from the interfacial lattice disorder in CdSe/CdS QDs.

The model proposed in Ref. [37], based on the observation of UCPL in CdTe colloidal QDs, suggests UCPL was generated by photon absorption between shallow surface electron and hole trapping states. In the model, the emission processes involve the thermally excited electron (hole) in the conduction band (valence band) radiatively recombining with the hole (electron) in the surface trapping states. According to this model, the following PL properties should be expected: First, UCPL intensity should decrease as the shell thickness increases since the QDs' surfaces are spatially farther away from their cores, leading to less overlap between the intrinsic band states and the surface trapping states. Second, the size dependence of UCPL should be much less pronounced than that of HPL, as surface states are typically less size sensitive than QDs' intrinsic band gap. Third, the possibility of having both the electron and hole recombined radiatively from the QDs' intrinsic states is determined by the thermal population of both carriers. When applied to our sample, by assuming the electron and hole trapping states are equally spaced, about 50 meV from the QDs' conduction and valence bands, respectively, the chance of having both carriers thermally activated to the intrinsic band states is about 1/10 (at 293 K) the chance of having only one of them being populated. In our data we see the first expectation is confirmed [Fig. 4(b)], while the second [Fig. 4(a)] and third ones (Fig. 5) do not match our results. Regarding the last two points, the UCPL of our samples showed size dependence identical to their HPL, and as shown in Fig. 5, the PL intensities at the HPL peak are around 48.5% of the maximum regardless of the excitation energy. In conclusion, the UCPL observed in our CdSe/CdS QD samples cannot be well described by the existing models used in colloidal QDs. Thus, a different model is proposed

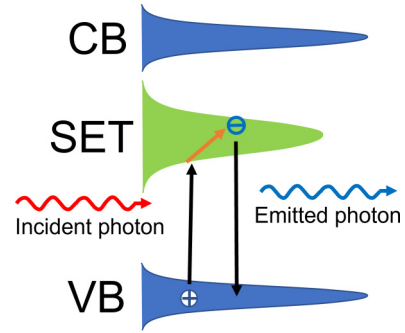


FIG. 6. Scheme of excitonic processes involved in the UCPL in CdSe/CdS QDs. CB: bottom of the QDs' intrinsic conduction band. VB: top of the QDs' intrinsic valence band. SET: shallow surface electron trapping states.

based on our experimental data to explain the UCPL processes inside CdSe/CdS QDs.

IV. MODEL FOR THE PL PROCESSES WITH SUBBAND EXCITATION

One of the key points in our proposed model is associated with the lack of the thermalization of electrons between conduction and trap states. Furthermore, the main mechanism of carrier thermalization within a band is by acoustic phonon coupling since longitudinal optical phonon coupling strength in CdSe QDs is much weaker than in bulk [29,49,50]. A possible candidate for energy states responsible for radiative recombination is the surface electron trapping state (SET) of CdS, which lies within 0.2 eV below CdS's intrinsic energy gap [51]. The shallow surface hole traps were not taken into account, as the main target of the shell growth and the final surface passivation with the CdFt monolayer is to remove surface hole traps, the major source of nonradiative decay processes [19,25]. Hence, the proposed mechanism is shown in Fig 6. Under SBE, in CdSe/CdS QDs, the photon absorption is achieved by an optical transition between the SET and the QDs' intrinsic valence band edge (VBE). Due to the poor overlap between the SET and VBE, this exciton has a very long lifetime (tens of nanoseconds [37]), allowing the electron to be thermalized inside the SET. Finally, the electron recombines with the hole left in the VBE through radiative or nonradiative decay processes. Following such a mechanism, the observed strong size dependence in the UCPL emission energy and the unusually high UCPL intensity observed in our samples can be properly explained. However, the model also suggests the UCPL decay lifetime is different from the band-edge emission, while in Fig. 2(c) a single exponential decay of 24 ns is prevalent, associated with only the band-edge recombination. Our explanation is that since the trapping efficiency of surface electronic states is much lower than the band-edge emission, the longer recombination times associated with these states is practically unobservable at high-energy excitation. Based on this model, the line shapes of both UCPL and down-conversion photoluminescence (DCPL) are determined by the thermalization processes inside the SET. In a more realistic case, the broad line shapes of QDs are produced by their size distribution, phonon-coupled PL processes, the

existence of other subband defect states, and other unknown processes. Therefore, mathematically, a Gaussian distribution $O_s(\varepsilon)$ with center ε_s and variance σ_s were assigned as the joint excitonic SDD for SET. They were determined by calculating the average value of the UCPL peak energies and FWHMs of the experimental data, respectively. To complete the overall line shape, three excitonic transition probabilities need to be defined: k_s , the intraband transition probability between the states inside the SET; k_r , the radiative decay probability; and k_{nr} , the nonradiative decay probability. For simplicity, all transition probabilities were considered to be energy independent. The mechanism for intraband transitions is considered to be an acoustic phonon-assisted carrier transfer, for which the transition rate is also modified by the phonons' SDD. For the sake of simplicity, the acoustic phonon dispersion relationship used is

$$\omega = ck,$$

where ω is the phonons' angular frequency, k denotes their wave number, and c denotes the speed of sound in the material. Although such an approximation does not provide a comprehensive description, it is sufficient to evaluate the physics behind the process. Therefore, in an n -dimensional system, the phonon's SDD is

$$g_n(\varepsilon) = C_g \left| \frac{\varepsilon^{n-1}}{e^{\varepsilon/k_B T} - 1} \right|, \quad (3)$$

where k_B is Boltzmann's constant and C_g is the coupling amplitude, which contains information about c and was set to 1, as it can be treated as a part of k_s . Thus, the time evolution of the excitonic density in the SET $N_s(\varepsilon)$ is

$$\begin{aligned} \frac{dN_s(\varepsilon)}{dt} &= \beta\delta(\varepsilon - \varepsilon_{ex}) - k_s \int_{\varepsilon - \varepsilon_c}^{\varepsilon + \varepsilon_c} g_n(\varepsilon' - \varepsilon) O_s(\varepsilon') d\varepsilon' N_s(\varepsilon) \\ &+ k_s \int_{\varepsilon - \varepsilon_c}^{\varepsilon + \varepsilon_c} g_n(\varepsilon - \varepsilon') N_s(\varepsilon') d\varepsilon' O_s(\varepsilon) - (k_r + k_{nr}) N_s(\varepsilon). \end{aligned} \quad (4)$$

The terms $\beta\delta(\varepsilon - \varepsilon_{ex})$ and $(k_r + k_{nr})N_s(\varepsilon)$ describe the photon absorption and emission processes, respectively, where β is the photon absorption rate and δ denotes the Dirac delta function. The second and third terms on the right side of Eq. (4) represent $N_s(\varepsilon)$ losing and receiving excitons through intraband transitions, respectively. Here ε_c denotes the phonon cutoff energy, not known for QDs at room temperature as the anharmonicity is significant, greatly expanding the phonon spectrum. Experimentally, a broad PL line shape was observed even at SBE. A ε_c value larger than 100 meV is required to describe the observed broadening, which is significantly larger than the phonon cutoff energy of the bulk material and is not currently well justified. Since 100 meV is significantly larger than $k_B T$, $g(\varepsilon)$ vanishes rapidly when ε_c is larger than the FWHM. To simplify the calculation, $\varepsilon_c \rightarrow \infty$ was used in the model. Under such an assumption,

$$k_s \int g_n(\varepsilon - \varepsilon') N_s(\varepsilon') d\varepsilon' \equiv k_s g_n \otimes N_s(\varepsilon), \quad (5)$$

the convolution between $g_n(\varepsilon)$ and $N_s(\varepsilon)$. By setting $\int g_n(\varepsilon' - \varepsilon) O_s(\varepsilon) d\varepsilon' \equiv F(\varepsilon)$, at steady state Eq. (4) becomes

$$0 = k_s O_s(\varepsilon) g_n(\varepsilon) \otimes N_s(\varepsilon) - [k_s F(\varepsilon) + k_r + k_{nr}] N_s(\varepsilon) + \beta\delta(\varepsilon - \varepsilon_{ex}). \quad (6)$$

In order to derive the expression for $N_s(\varepsilon)$, a few approximations were introduced to the calculation. When at most one exciton is present in the QD ($\beta \ll k_r$), the term $k_s O_s(\varepsilon) g_n(\varepsilon) \otimes N_s(\varepsilon)$ is always smaller than the term $k_s F(\varepsilon)$. Thus, $k_s O_s(\varepsilon) g_n(\varepsilon) \otimes N_s(\varepsilon)$ can be considered a correction to Eq. (6), and

$$N_s^0(\varepsilon) \approx \frac{\beta\delta(\varepsilon - \varepsilon_{ex})}{k_s F(\varepsilon) + k_r + k_{nr}}. \quad (7)$$

The superscript 0 denotes the unmodified solution to Eq. (6). Then $N_s(\varepsilon)$ can be solved iteratively by substituting Eq. (7) into Eq. (6),

$$0 = k_s O_s(\varepsilon) g_n(\varepsilon) \otimes N_s^0(\varepsilon) - [k_s F(\varepsilon) + k_r + k_{nr}] N_s^1(\varepsilon) + \beta\delta(\varepsilon - \varepsilon_{ex}). \quad (8)$$

In general, for any integer $m > 0$, $N_s^m(\varepsilon)$ satisfies

$$0 = k_s O_s(\varepsilon) g_n(\varepsilon) \otimes N_s^{m-1}(\varepsilon) - [k_s F(\varepsilon) + k_r + k_{nr}] N_s^m(\varepsilon) + \beta\delta(\varepsilon - \varepsilon_{ex}). \quad (9)$$

The attempt to fit n started by treating the phonon modes inside the QDs as identical to the ones in bulk materials, a three-dimensional system. Under this assumption,

$$g_3(\varepsilon) = C_g \left| \frac{\varepsilon^2}{e^{\varepsilon/k_B T} - 1} \right| \quad (10)$$

was plugged into the model.

As shown in Figs. 7(a) and 7(b), the recurrence converges as m increases. Meanwhile, as expected, a slower converging speed was observed with smaller k_r/k_s value. The simulation's k_r/k_s dependence is shown in Fig. 7(c), where UCPL (DCPL) processes are slightly reduced (increased) as k_r/k_s decreases, indicating a longer radiative decay lifetime. As $k_r/k_s \rightarrow 0$, it is invalid to treat $k_s O_s(\varepsilon) g_n(\varepsilon) \otimes N_s(\varepsilon)$ as a correction anymore. As k_r/k_s decreases, the iteration itself could be understood as resembling the thermalization process. From the numerical calculation standpoint, the computation time increases too fast as the number of iterations increases; consequently, our calculations stopped when $k_r/k_s = 0.1$. The simulation result is shown in Fig. 7(d), where the fitting was done by adjusting the joint width of the SET and VB bands, indicating a good resemblance to the experimental data. The relatively low intraband transition rate can be understood as a poor bulk-phonon-mediated transition between the SET and CB states, compounded by the reduced mobility of the surface carrier due to the surface passivation treatment.

In the investigation of the model's excitation energy dependence, the simulated PL line shape is very insensitive to the change in ε_{ex} [Fig. 8(a)]. Different from the experimental data, where a slight redshift of the samples' PL spectra was observed as ε_{ex} decreased, a negligible change was suggested by the simulation results. This difference can be understood as the QD ensemble's PL line shape being convoluted by their size distribution, leading to a redshift of the UCPL peak with

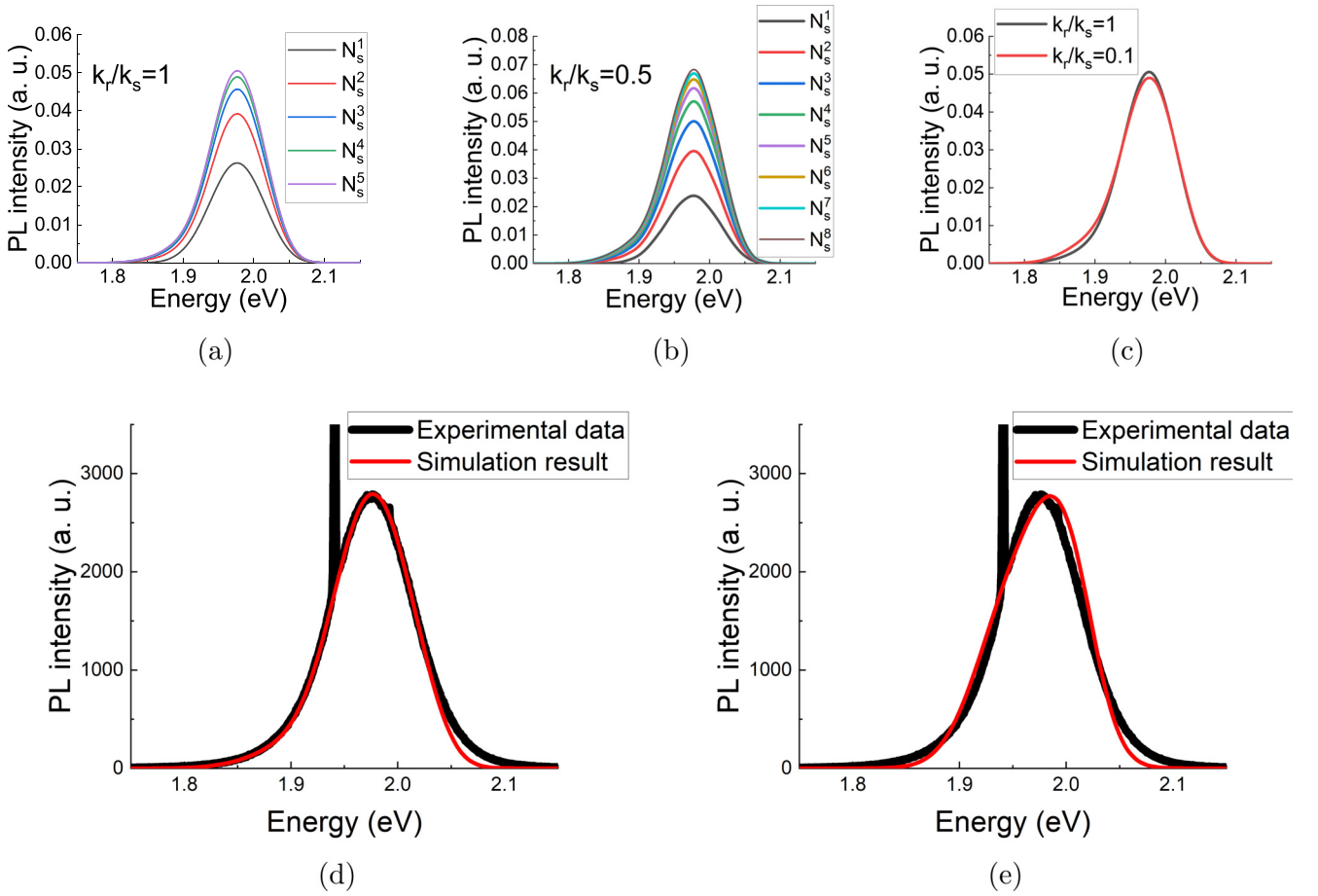


FIG. 7. Simulated PL spectra with (a) $k_r/k_s = 1$ and (b) $k_r/k_s = 0.5$, where an increased intensity indicates a larger iteration step. (c) Fully iterated PL spectra with $k_r/k_s = 1$ and $k_r/k_s = 0.1$. (d) and (e) show simulation results (thin lines) fitted to the experimental data (thick lines, obtained from sample 3 with $\varepsilon_{\text{ex}} = 1.935$ eV) with (d) $n = 3$, $\varepsilon_s = 1.976$ eV, and $\sigma_s = 38$ meV (FWHM = 89 meV) and (e) $n = 2$, $\varepsilon_s = 2.000$ eV, and $\sigma_s = 34$ meV (FWHM = 80 meV). In both simulations $\beta/k_t = 0.01$ (ensuring the excitonic density is less than 1).

decreased ε_{ex} . This effect is suppressed when lowering the excitation energy, as fewer QDs (only the largest ones) participate in the PL processes, leading to a PL spectral narrowing [52]. The experimental data are shown in Fig. 8(b) (the PL

intensity is plotted in logarithmic scale as it decreases rapidly when ε_{ex} decreases); the redshift of the UCPL peak energy gradually stops as ε_{ex} decreases. This is a strong indication that the model resembles the UCPL processes in QDs. One

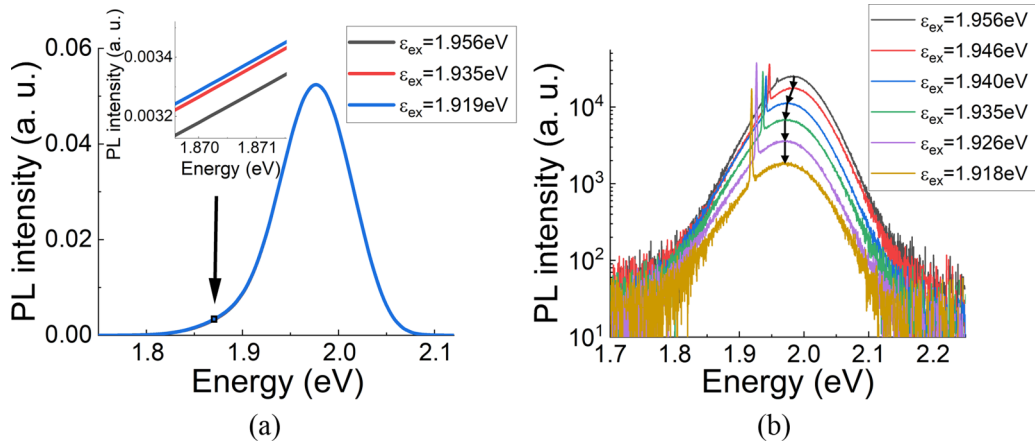


FIG. 8. (a) Simulated PL spectra (ninth iteration) with $\varepsilon_{\text{ex}} = 1.956$ eV (bottom), 1.919 eV (middle) and 1.919 eV (top); the inset is a close-up view of the small rectangular area. (b) PL spectra of the sample with $\varepsilon_{\text{ex}} = 1.956$ eV, 1.945 eV, 1.938 eV, 1.929 eV and 1.919 eV (from top to bottom).

more fact that needs to be pointed out is that Fig. 8(b) also suggests that a deep trap emission is not observable even at SBE, further suggesting the lack of defects in the cores.

The case where the thermalization processes is mainly due to surface phonons was also tested, using $n = 2$ in Eq. (3),

$$g_2(\varepsilon) = C_g \left| \frac{\varepsilon}{e^{\varepsilon/k_B T} - 1} \right|. \quad (11)$$

With the two-dimensional (2D) phonon mode, the predetermined ε_s and σ_s values were not able to reproduce the experimental results. They have to be treated as fitting parameters, and a higher $\varepsilon_s \approx 2.000$ eV and a narrower $\sigma_s \approx 34$ meV are required in the simulation, regardless of the value of k_r/k_s . Such an observation suggests that if both three-dimensional (3D) and 2D phonon modes are coupled in the QDs' PL processes at SBE, they will peak at different energies. In the calculation of χ^2 [defined as $\chi^2 = \sum \frac{[I_s(\varepsilon) - I_e(\varepsilon)]^2}{I_e(\varepsilon)}$, where $I_s(\varepsilon)$ and $I_e(\varepsilon)$ denote the PL intensity at energy ε obtained with the simulated result and experimental data, respectively; the integrated PL intensities were normalized to unity before the calculation was run], the 3D model ($\chi^2 \approx 0.044$) was found to be slightly better than the 2D model ($\chi^2 \approx 0.062$). However, as shown in Fig. 7(e), the fitting result produced with the 2D model is noticeably worse than the 3D ones. In conclusion, although the existence of surface phonon coupled processes cannot be completely excluded, our model suggests that they are not the major processes to produce UCPL in CdSe/CdS QDs.

Another important part is the nonradiative decay rate k_{nr} , which mathematically cannot be distinguished with k_r in our model. A larger k_{nr} value, which is equivalent to lowering the QY, will change the PL strength but not the line shape. Therefore, our model cannot provide QY information for the transitions generating the UCPL in CdSe/CdS QDs. However, experimentally, we have observed similar enhancement in the PL strength with both high-energy and subband excitations after passivating the CdS shell with CdFt (PL intensity increased roughly by a factor of 3 in both tests). Such evidence strongly suggests that the transition between SET and the QDs' valence band is optically active and has transition strength comparable to the band-edge emission. This property of surface states in CdSe QDs was reported in the study by Voznyy [53], the trap-LUMO (LUMO: lowest unoccupied molecular orbital) and HOMO-LUMO (HOMO: highest occupied molecular orbital) were both optical allowed and have comparable transition strengths at room temperature. Because zinc-blende CdSe and zinc-blende CdS have almost identical crystal structures, it is reasonable to expect the SET on the CdS shell to have similar behavior. The nonradiative decay processes are significantly enhanced by the deep trapping states, which not only can hold the excitons but also provide much smaller energy differences than the QDs' band gap, favoring excitonic recombination through cascade phonon emission processes. Since the deep trapping states were removed during the passivation processes, the SET does not favor nonradiative decay processes.

In conclusion, except for the UCPL high-energy tail, the model provides robust predictions of the PL line shape. Such disagreement could possibly be due to the oversimplification of the model in that no exciton detrapping processes (electron

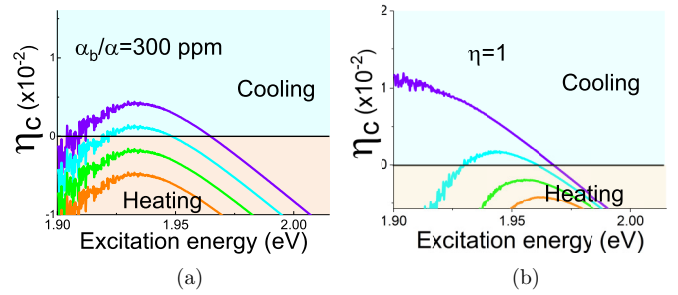


FIG. 9. Estimated cooling efficiency of sample 2 as a function of ε_{ex} . (a) From top to bottom: $\eta = 1, 0.997, 0.994$, and 0.991 . (b) From top to bottom: $\frac{\alpha_b}{\alpha} = 100, 500, 1000$, and 1500 ppm. α is obtained from the absorption spectrum.

detrapping from the SET to the conduction band) are considered. Since the difference of the ill-fit high-energy tail is insignificant compared to the overall line shape and would eventually lead to an underestimation of the net energy UC, the simulated PL intensity spectrum $I(\varepsilon)$ can be used to calculate the mean emission energy $\bar{\varepsilon}_{em}$, given by

$$\bar{\varepsilon}_{em} = \frac{\int_0^\infty \varepsilon I(\varepsilon) d\varepsilon}{\int_0^\infty I(\varepsilon) d\varepsilon}, \quad (12)$$

where $\int_0^\infty \varepsilon I(\varepsilon) d\varepsilon$ denotes the total emission power and $\int_0^\infty I(\varepsilon) d\varepsilon$ denotes the total emission rate. Plugging the result of Eq. (12) into Eq. (1), η_c can be obtained. Figure 9 shows the results for sample 2's possible cooling efficiency with different QYs η and background absorption strengths $\frac{\alpha_b}{\alpha}$, predicting a cooling zone. The calculation also suggests that unless the background absorption is very small, a maximum of η_c is found around 1.94 eV. Since the synthesis method used for our QDs samples is supposed to yield almost unity QY and it is supported by all experimental data, a net cooling effect might have already taken place during the experiment.

V. CONCLUSIONS

UCPL spectra of zinc-blende CdSe/CdS QDs were obtained with SBE. The experimental data suggested that the PL processes were mainly due to optical transitions between the SET and VBE, while the energy UC was achieved through thermalization processes within the dispersed SET. Therefore, a net energy UC is, in principle, achievable by exciting the QDs at the tail of their SET. Based on experimental data, a semiempirical model describing the PL processes was constructed. The simulated results show extraordinary agreement with the experimental data and further indicate that the broadening of zinc-blende CdSe QDs' UCPL spectra is mainly due to the strong coupling between the photon-induced exciton and the "bulk" acoustic phonon modes. They also suggest that surface passivation reduces excitons' mobility in the surface band. Although the large cutoff phonon energy cannot yet be explained, quantitative predictions can be produced by the model. With the model's help, the possible cooling efficiency in CdSe QDs was calculated, showing the possibility of realizing OR in high-quality zinc-blende CdSe QDs.

ACKNOWLEDGMENTS

We want to thank Dr. D. Minner, who provided generous practical suggestions on QD synthesis, and Dr. B. Ray, who helped us construct the synthesis equipment. We also want

thank Prof. Vemuri in our department, who kindly provided helpful advice on orienting the paper structure. R.S.D. acknowledges support from the National Science Foundation through Grant No. PHY-1607360 and technical support from the IUPUI Integrated Nanosystem Development Institute.

-
- [1] P. Pringsheim, *Z. Phys.* **57**, 739 (1929).
- [2] R. I. Epstein, M. I. Bucwald, B. C. Edwards, T. R. Gosnell, and C. E. Mungan, *Nature (London)* **377**, 500 (1995).
- [3] J. L. Clark and G. Rumbles, *Phys. Rev. Lett.* **76**, 2037 (1996).
- [4] C. E. Mungan, M. I. Buchwald, B. C. Edwards, R. I. Epstein, and T. R. Gosnell, *Phys. Rev. Lett.* **78**, 1030 (1997).
- [5] S. R. Bowman and C. E. Mungan, *Appl. Phys. B* **71**, 807 (2000).
- [6] A. Mendioroz, J. Fernández, M. Voda, M. Al-Saleh, R. Balda, and A. J. García-Adeva, *Opt. Lett.* **27**, 1525 (2002).
- [7] C. W. Hoyt, M. P. Hasselbeck, M. Sheik-Bahae, R. I. Epstein, S. Greenfield, J. Thiede, J. Distel, and J. Valencia, *J. Opt. Soc. Am. B* **20**, 1066 (2003).
- [8] M. Sheik-Bahae and R. I. Epstein, *Phys. Rev. Lett.* **92**, 247403 (2004).
- [9] S. Bigotta, D. Parisi, L. Bonelli, A. Toncelli, M. Tonelli, and A. Di Lieto, *J. Appl. Phys.* **100**, 013109 (2006).
- [10] J. Fernandez, A. J. Garcia-Adeva, and R. Balda, *Phys. Rev. Lett.* **97**, 033001 (2006).
- [11] W. Patterson, S. Bigotta, M. Sheik-Bahae, D. Parisi, M. Tonelli, and R. Epstein, *Opt. Express* **16**, 1704 (2008).
- [12] Q. Zhang, J. Zhang, M. I. B. Utama, B. Peng, M. de la Mata, J. Arbiol, and Q. Xiong, *Phys. Rev. B* **85**, 085418 (2012).
- [13] A. Ekimov, A. Efros, and A. Onushchenko, *Solid State Commun.* **56**, 921 (1985).
- [14] V. I. Klimov, A. A. Mikhailovsky, S. Xu, A. Malko, J. A. Hollingsworth, C. A. Leatherdale, H.-J. Eisler, and M. G. Bawendi, *Science* **290**, 314 (2000).
- [15] R. Azmi, S. Oh, and S. Jang, *ACS Energy Lett.* **1**, 100 (2016).
- [16] L. Zan, D. Lin, P. Zhong, and G. He, *Opt. Express* **24**, 7643 (2016).
- [17] N. Chestnoy, T. D. Harris, R. Hull, and L. E. Brus, *J. Phys. Chem.* **90**, 3393 (1986).
- [18] M. Califano, A. Franceschetti, and A. Zunger, *Nano Lett.* **5**, 2360 (2005).
- [19] A. Veamatahau, B. Jiang, T. Seifert, S. Makuta, K. Latham, M. Kanehara, T. Teranishi, and Y. Tachibana, *Phys. Chem. Chem. Phys.* **17**, 2850 (2015).
- [20] S. Singh, R. Tomar, S. ten Brinck, J. De Roo, P. Geiregat, J. C. Martins, I. Infante, and Z. Hens, *J. Am. Chem. Soc.* **140**, 13292 (2018).
- [21] H. Zou, C. Dong, S. Li, C. Im, M. Jin, S. Yao, T. Cui, W. Tian, Y. Liu, and H. Zhang, *J. Phys. Chem. C* **122**, 9312 (2018).
- [22] X. Wang, L. Qu, J. Zhang, X. Peng, and M. Xiao, *Nano Lett.* **3**, 1103 (2003).
- [23] C. de Mello Donegá, M. Bode, and A. Meijerink, *Phys. Rev. B* **74**, 085320 (2006).
- [24] I. Coropceanu, A. Rossinelli, J. R. Caram, F. S. Freyria, and M. G. Bawendi, *ACS Nano* **10**, 3295 (2016).
- [25] C. Pu and X. Peng, *J. Am. Chem. Soc.* **138**, 8134 (2016).
- [26] W. Nan, Y. Niu, H. Qin, F. Cui, Y. Yang, R. Lai, W. Lin, and X. Peng, *J. Am. Chem. Soc.* **134**, 19685 (2012).
- [27] L. Brus, *J. Phys. Chem.* **90**, 2555 (1986).
- [28] N. Mori and T. Ando, *Phys. Rev. B* **40**, 6175 (1989).
- [29] M. C. Klein, F. Hache, D. Ricard, and C. Flytzanis, *Phys. Rev. B* **42**, 11123 (1990).
- [30] A. L. Efros, *Phys. Rev. B* **46**, 7448 (1992).
- [31] A. L. Efros and M. Rosen, *Phys. Rev. Lett.* **78**, 1110 (1997).
- [32] A. M. Kelley, *J. Phys. Chem. Lett.* **1**, 1296 (2010).
- [33] M. Ye and P. C. Se arson, *Phys. Rev. B* **84**, 125317 (2011).
- [34] M. Grabolle, M. Spieles, V. Lesnyak, N. Gaponik, A. Eychmüller, and U. Resch-Genger, *Anal. Chem.* **81**, 6285 (2009).
- [35] O. E. Semonin, J. C. Johnson, J. M. Luther, A. G. Midgett, A. J. Nozik, and M. C. Beard, *J. Phys. Chem. Lett.* **1**, 2445 (2010).
- [36] O. Chen, J. Zhao, V. P. Chauhan, J. Cui, C. Wong, D. K. Harris, H. Wei, H.-S. Han, D. Fukumura, R. K. Jain, and M. G. Bawendi, *Nat. Mater.* **12**, 445 (2013).
- [37] X. Wang, W. W. Yu, J. Zhang, J. Aldana, X. Peng, and M. Xiao, *Phys. Rev. B* **68**, 125318 (2003).
- [38] K. I. Rusakov, A. A. Gladyschuk, Y. P. Rakovich, J. F. Donegan, S. A. Filonovich, M. J. M. Gomes, D. V. Talapin, A. L. Rogach, and A. Eychmüller, *Opt. Spectrosc.* **94**, 859 (2003).
- [39] E. Poles, D. C. Selmarten, O. I. Mičić, and A. J. Nozik, *Appl. Phys. Lett.* **75**, 971 (1999).
- [40] D. F. Underwood, T. Kippeny, and S. J. Rosenthal, *J. Phys. Chem. B* **105**, 436 (2001).
- [41] Y. Rakovich, S. Filonovich, M. Gomes, J. Donegan, D. Talapin, A. Rogach, and A. Eychmüller, *Phys. Status Solidi B* **229**, 449 (2002).
- [42] C. R. Bullen and P. Mulvaney, *Nano Lett.* **4**, 2303 (2004).
- [43] O. Chen, X. Chen, Y. Yang, J. Lynch, H. Wu, J. Zhuang, and Y. Cao, *Angew. Chem., Int. Ed.* **47**, 8638 (2008).
- [44] K. Manthiram, B. J. Beberwyck, D. V. Talapin, and A. P. Alivisatos, *J. Visualized Exp.* **82**, e50731 (2013).
- [45] M. Hua, Optical refrigeration on CdSe/CdS quantum dots, Ph.D. thesis, Purdue University, 2019.
- [46] R. Karel Čapek, I. Moreels, K. Lambert, D. De Mynck, Q. Zhao, A. Van Tomme, F. Vanhaecke, and Z. Hens, *J. Phys. Chem. C* **114**, 6371 (2010).
- [47] Y. A. Yang, H. Wu, K. R. Williams, and Y. C. Cao, *Angew. Chem., Int. Ed.* **44**, 6712 (2005).
- [48] S. Fengler, E. Zillner, and T. Dittrich, *J. Phys. Chem. C* **117**, 6462 (2013).

- [49] A. P. Alivisatos, T. D. Harris, P. J. Carrol, M. L. Steigerwald, and L. E. Brus, *J. Chem. Phys.* **90**, 3463 (1989).
- [50] A. M. Kelley, Q. Dai, Z. Jiang, J. A. Baker, and D. F. Kelley, *Chem. Phys.* **422**, 272 (2013).
- [51] J. D. Levine and P. Mark, *Phys. Rev.* **144**, 751 (1966).
- [52] D. J. Norris and M. G. Bawendi, *J. Chem. Phys.* **103**, 5260 (1995).
- [53] O. Voznyy, *J. Phys. Chem. C* **115**, 15927 (2011).